JET–P(98)32

D Testa et al

Measurement and Interpretation of Interaction of MeV Energy Protons with Lower Hybrid Waves in JET Plasmas

JET–P(98)32

Measurement and Interpretation of Interaction of MeV Energy Protons with Lower Hybrid Waves in JET Plasmas

D Testa[1], C N Lashmore-Davies[2], A Gondhalekar,
L-G Eriksson, M Mantsinen[3], T J Martin[2].

JET Joint Undertaking, Abingdon, Oxfordshire, OX14 3EA,
[1]Imperial College of Science, Technology and Medicine, London, SW7 2BZ, UK.
[2] UKAEA Fusion, Culham Science Centre, Abingdon, OX14 3DB, UK.
(UKAEA/Euratom Fusion Association)
[3] Helsinki University of Technology, Association Euratom, Tekes, Espoo, Finland.

Preprint of a Paper to be submitted for publication in
Plasma Physics and Controlled Fusion

September 1998

ABSTRACT

Experiments with simultaneous lower hybrid current drive and ion cyclotron resonance frequency heating of minority protons in JET deuterium plasmas showed efficient coupling of LH power to the MeV energy anisotropic protons. Such interaction represents parasitic loss of LH power, intended for electron current drive, to the proton population, with important implications for the efficiency of LH current drive schemes in fusion devices containing high energy charged fusion products. We solve the hot-plasma dispersion relation in the LH range of frequencies for plasmas containing high energy minority anisotropic protons and electrons, and find that multiple solutions of the dispersion relation with perpendicular refractive index $n_\perp>40$ exist in the plasma centre due to the presence of the protons. These hot-plasma modes give ≈20%-40% damping of LH input power onto the protons by perpendicular Landau damping. Combinations of background plasma and LH antenna parameters exist for which no solutions of the LH dispersion relation are found with $n_\perp\geq20$, thus reducing damping of LH power to the protons to ≈5%-10%. This suggests ways of reducing the parasitic loss of LH power to high energy charged fusion products.

I. INTRODUCTION

Measurements using a Neutral Particle Analyser (NPA) have yielded the energy distribution function of protons in the range $0.3\leq E(MeV)\leq1.1$ in the Joint European Torus (JET) [1,2]. The protons, a minority ion species in deuterium plasmas, are driven to MeV energies by Ion Cyclotron Resonance Frequency (ICRF) heating, and their distribution function $f_p(E)$ is strongly anisotropic for energies $E>>E_{CRIT}$, where E_{CRIT} is the critical energy at which the proton-electron and proton-ion slowing-down time are equal [3]. The NPA measurement set-up and details of deduction of the energy distribution function are given in [2]. For $E>E_{CRIT}$ the proton distribution function may be approximated by a bi-Maxwellian. Then the perpendicular temperature and density of the proton population in the plasma centre can be deduced from the NPA measurements [4,5].

During simultaneous Lower Hybrid Current Drive (LHCD) and minority ICRF heating of protons, the NPA measurements showed efficient coupling of LH power to the high energy anisotropic proton population. The coupling was deduced for driven as well as for slowing-down protons. Perpendicular Landau damping [6] enables LH waves to couple energy to ions if the resonance condition $\upsilon_\perp>\upsilon_{THR}=c/n_{\perp MAX}$ is satisfied. Here $n_{\perp MAX}$ is the maximum perpendicular refractive index in the LH spectrum and υ_{THR} is the minimum perpendicular velocity for wave-particle resonance. The observed interaction is contrary to expectations in two respects: (a) taking place in the whole energy range of the measurements, it suggested that $n_{\perp MAX}\geq40$, whereas conventional model calculations in JET of LH dispersion under pertinent conditions

give $n_{\perp MAX} \leq 20$ [7,8]; and (b) from the measurements we deduced that $\approx 30\%$ of applied LH power was coupled to the protons, much exceeding the predictions of $\approx 5\%$-10%, based on $n_{\perp MAX} \leq 20$ [7,9].

This paper is organised as follows. In Section 2 we present measurements of ICRF-driven protons during LHCD. In Section 3 we derive from the measurements the fraction of LH power damped by the protons. In Section 4 we present numerical simulations of the perpendicular proton distribution function, showing that an up-shifted perpendicular refractive index $n_{\perp MAX} \geq 40$ could produce the observed absorption of LH power by the protons. In Section 5 we solve the dispersion relation in the LH range of frequencies for plasmas containing high energy anisotropic minority proton and electron populations. This shows that the required up-shift in $n_\perp$ takes place in the centre of JET plasmas due to the protons. Then in Section 6 we compute the fraction of input LH power coupled to the proton population. Section 7 summarises our conclusions.

II. EXPERIMENTAL EVIDENCE OF ABSORBTION OF LH POWER BY HIGH ENERGY PROTONS

Early observations in JET [9] showed qualitatively the possibility of interaction of LH waves with high energy protons, but no direct measurements were made of $f_p(E)$. To establish experimental evidence for coupling of LH wave power to the protons we analysed $f_p(E)$ for 74 plasma pulses, 24 with ICRF and LH heating power applied simultaneously and 50 with ICRF heating power alone. Plasma pulses with ICRF heating alone have been used to establish the comparison for those in which LH power was superimposed to ICRF heating. The pulses analysed here span the range in central electron density $1.3 < n_{e0}(10^{19} m^{-3}) < 4.7$, central electron temperature $3.6 < T_{e0}(keV) \leq 7.2$, toroidal magnetic field on axis $2.6 < B\phi_0(T) < 3.4$ and plasma current $1 < I\phi(MA) < 3$, with ICRF and LH power $P_{ICRF} \leq 9.5MW$ and $P_{LH} \leq 4.6MW$.

Clearest evidence of interaction between the protons and LH waves is obtained when LH waves are acting on the slowing-down proton population. Figs.1a and 1b show comparison of a pulse with ICRF heating alone with one having ICRF and LH power applied simultaneously, the proton-electron slowing down time τ_{SD} being equal in the two pulses. In Fig.1a we notice that with ICRF heating alone the hydrogen flux to the NPA decays within the slowing-down time scale after termination of ICRF heating. On the other hand, with simultaneous ICRF and LH heating as in Fig.1b, the hydrogen flux is sustained for a longer time when the LH pulse extends beyond the ICRF pulse. Thus these measurements show direct absorption of LH wave power by the protons, sustaining flux and temperature of the proton population well above the expected slowing-down level after termination of ICRF heating. This behaviour is seen in different plasmas with respect to the toroidal magnetic field and current, electron density and temperature, provided a sufficient amount of LH power, $P_{LH} \geq 1MW$, is coupled to the plasma.

Usual simulations of LHCD in JET plasmas [7,8,9] omit the fast ion populations and predict that only protons with perpendicular energy $W_{\perp} \geq E_{THR} = m_p c^2 / 2n^2_{\perp MAX} \approx 1.2MeV$, would interact with LH waves. NPA measurements of $f_p(E)$ show that the proton population is sustained by LH waves in the whole energy range, $E \geq 287keV$. Thus, in contrast to expectations, we deduce that the energy threshold for interaction between the protons and LH waves is much lower than that predicted by usual simulations of LHCD in JET plasmas. We attribute the observed interaction to modification of the LH wave spectrum in the plasma centre due to the presence of the proton population.

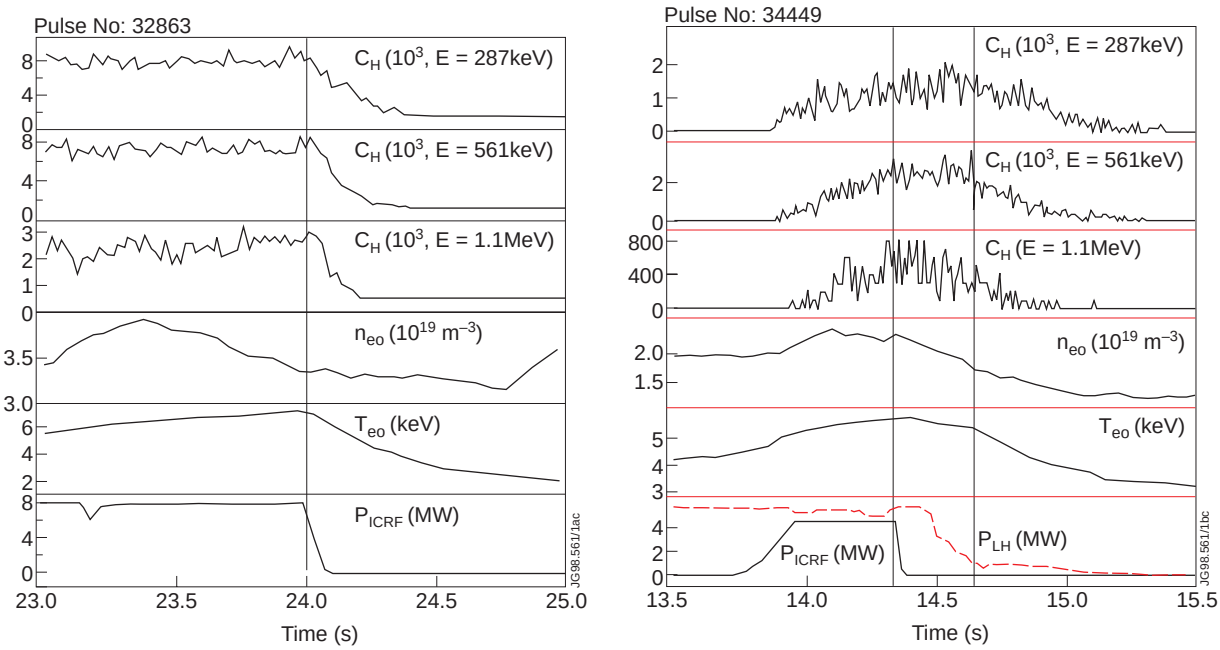

Figure 1. Time evolution of count rate (C_H) for H-atoms measured by the NPA, central electron density (n_{e0}) and temperature (T_{e0}), input power (P_{ICRF} and P_{LH}) during on-axis D(H) minority ICRF heating. In Fig.1a, for a pulse with $B_{\phi 0}$=2.8T, I_{ϕ}=1.25MA and central proton density $n_{p0}=8.2 \times 10^{17} m^{-3}$, we notice that after switching-off ICRF heating the high energy H-flux decays over $\tau \approx \tau_{SD}$. In Fig.1b, for a pulse with $B_{\phi 0}$=3T, I_{ϕ}=3MA and $n_{p0}=2.8 \times 10^{17} m^{-3}$, we notice that the atomic flux is constant with time and sustained by LH waves for $\tau \approx 0.5 \tau_{SD}$ after ICRF power is terminated. $\tau_{SD} \approx 0.6$s is equal in the two plasma pulses.

III. DEDUCTION OF ABSORBED LH POWER

During ICRF heating of minority protons in deuterium plasmas the proton distribution function becomes strongly anisotropic for energies $E >> E_{CRIT}$ [3], where $E_{CRIT} = 14.8 A_p T_e [\Sigma n_j Z_j^2 / n_e A_j]^{2/3} \approx 8.7 T_e$ is the critical energy at which the proton-electron and proton-ion collision frequencies are equal. The energy range of the NPA measurements lies well above E_{CRIT}, and $f_p(E)$ is well described with a bi-Maxwellian of the form

$$f(\upsilon_{||}, \upsilon_{\perp}) = \left(\frac{m}{2\pi} \right)^{3/2} \frac{n}{T_{||}^{1/2} T_{\perp}} exp\left(-\frac{\upsilon_{||}^2}{u_{||}^2} - \frac{\upsilon_{\perp}^2}{u_{\perp}^2} \right). \quad (1)$$

Here $u_{||,\perp}=(2T_{||,\perp}/m)^{1/2}$ are respectively the parallel and perpendicular thermal speeds and $T_\perp >> T_{||}$. The total energy content of such distribution function is $W=n_p(T_{p\perp}+T_{||}/2)$. For ICRF-driven protons the perpendicular energy is determined by the balance between the coercive force of the ICRF wave field and the collisional drag on thermal electrons, giving $W_p \approx W_{p\perp}=n_p T_{p\perp}=\rho_{ICRF}\tau_{SD}/2$, where ρ_{ICRF} is the ICRF power density coupled to the protons.

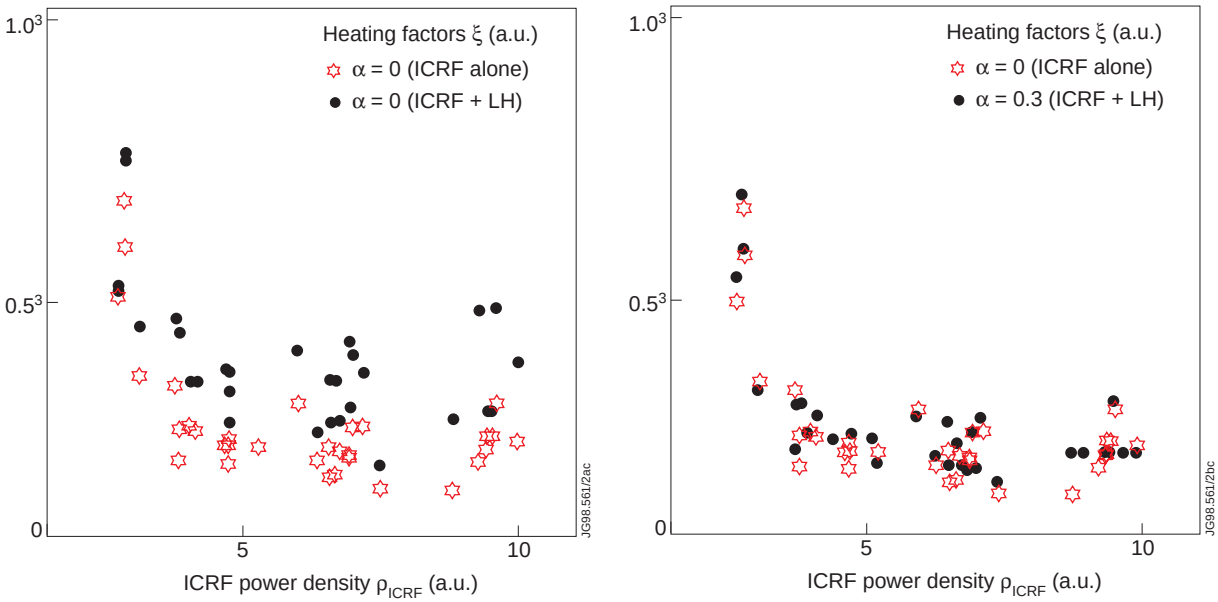

Figure 2. Comparison of ξ *for ICRF heating alone and ICRF+LH heating. Fig.2a shows that during combined ICRF+LH heating* ξ *is well in excess of that for ICRF heating alone if only ICRF power is considered for proton heating, obtaining a correlation coefficient* R=0.75. *Fig.2b shows that to reconcile the magnitude of* ξ *for these two heating schemes we need* ≈30% *of LH power added to ICRF power, obtaining a correlation coefficient* R=0.97±0.01.

We determine the fraction of LH power coupled to the protons by comparing ion heating in pulses with ICRF alone with those with ICRF+LH power. In order to normalise with respect to variations in other variables, such as proton-electron slowing-down time, proton density and applied power, we use as a figure-of-merit for proton heating the factor $\xi=n_p T_{p\perp}/\rho_{TOT}\tau_{SD}$, where $\rho_{TOT}=\rho_{ICRF}+\alpha\rho_{LH}$ is the total wave power density coupled to the protons. We wish to determine α, the fraction of LH wave power directly absorbed by the protons. Here α ranges from 0 to 1 corresponding to limiting cases of none to all LH wave power coupled to the protons. We determine ξ by averaging the measurements over 200ms during the steady state heating phase of the plasma pulses. In Fig.2a we show two groups of data, pulses with ICRF power alone and those having ICRF+LH power for the same value of ρ_{ICRF}. Entries in our data set have different values of ρ_{LH}, and therefore Fig.2a. shows large scatter in the data. We estimate the uncertainty in ξ*~20%*, mainly due to uncertainties in the proton density: thus we need to investigate systematic trends in the measurements and we cannot rely simply on a pulse-to-pulse comparison. We then iterate α to obtain the best correlation in the whole data set, as shown in Fig.2b.

We use a least-squares method with confidence level 0.95 to deduce the best fit α to the heating factor ξ comparing ICRF alone and ICRF+LH data. The correlation R between two sets

of data *(X,Y)* is defined as $R(X,Y)=Cov(X,Y)/\sigma_X\sigma_Y$: here *Cov(X,Y)* is the covariance, σ_X and σ_Y are the standard deviations. Fig.2a shows the results of using $\alpha=0$ whereby we obtain $R=0.75$. Maximum value of $R=0.97\pm0.01$ is obtained with $\alpha=0.3\pm0.05$, the corresponding result is shown in Fig.2b. We therefore conclude that on the average $\approx 30\%$ of LH wave power is directly damped by the protons, over a wide range in background plasma parameters and input ICRF and LH wave power.

IV. SIMULATIONS OF PROTON DISTRIBUTION FUNCTION

To investigate the effect of LH wave power absorption on the proton distribution function we have adopted Stix's model for ICRF heating [3], which considers a balance between the coercive force of waves and the collisional drag on the heated ions. This model has been extended in [10] to the case of ion heating in a combined wave field of ICRF+LH. Following [10], a 1D Fokker Planck equation in velocity space is constructed for the minority fast ion population including the quasilinear (QL) diffusion coefficients describing ICRF (D_{ICRF}) and LH (D_{LH}) heating and collisional thermalisation with the bulk plasma (C_{SD}). The equation is derived reducing the original 3D velocity co-ordinate system ($\upsilon_{||},\upsilon_{\perp},\phi$) to a 1D problem by assuming toroidal symmetry, expanding the distribution function in Legendre polynomials in the pitch-angle $\mu=\upsilon_{||}/\upsilon_{\perp}$ and zero-order averaging over μ. Thus the only velocity co-ordinate surviving is υ. This procedure gives the time-dependent QL evolution equation in velocity space for the minority fast ion perpendicular distribution function

$$\frac{\partial f_0}{\partial t}=\frac{1}{\tau_{SD}\upsilon^2}\frac{\partial}{\partial\upsilon}\left[C_{SD}+\upsilon^2\tau_{SD}\left(D_{ICRF}+D_{LH}\right)\frac{\partial}{\partial\upsilon}\right]f_0\,, \tag{2}$$

where the QL diffusion operators in velocity space are

$$C_{SD}=\frac{T_i}{m_i\upsilon}\left(\upsilon_C^3+\frac{T_e}{T_i}\upsilon^3\right)\frac{\partial}{\partial\upsilon}+\left(\upsilon_C^3+\upsilon^3\right), \tag{2a}$$

$$D_{ICRF}=\frac{\pi Z^2e^2}{4m^2\Omega}\sum_{q=0}^{\infty}\left|\Psi_+J_{q-1}\left(\frac{k_\perp\upsilon_\perp}{\Omega}\right)+\Psi_-J_{q+1}\left(\frac{k_\perp\upsilon_\perp}{\Omega}\right)\right|^2\,, \tag{2b}$$

$$D_{LH}=\frac{\pi Z^2e^2}{4m^2\omega_{LH}}\frac{c^3}{\upsilon^3}\int dn_{||}\,\frac{\left|\Psi(n_{||})\right|^2}{n_\perp^3(n_{||})}H\left[1-\frac{c^3}{\upsilon^3n_\perp^3(n_{||})}\right]. \tag{2c}$$

Here m_i and T_i are the majority ion mass and temperature, $\upsilon_C=(2E_{CRIT}/m)^{1/2}$, Z, m and Ω are the minority ion charge, mass and cyclotron angular frequency, Ψ_+ and Ψ_- are the amplitudes of the left and right hand circularly polarised component of the ICRF wave field, $k_\perp$ is the

perpendicular wavenumber and $\left|\Psi\left(n_{||}\right)\right|^2$ is the LH wave energy density spectrum. H is the step function and $J_{q\pm1}$ are Bessel functions of first kind. When stationary solution ($\partial/\partial t=0$) in the high velocity limit ($\upsilon >> \upsilon_C$) are considered, equation 2 is integrated straightforwardly to give

$$f_0(\upsilon) = f_0(\upsilon_0) exp\left(-\frac{1}{\tau_{SD}} \int_{\upsilon_0}^{\upsilon} \frac{\upsilon d\upsilon}{D_{ICRF} + D_{LH}} \right). \qquad (3)$$

Here υ_0 is the lowest velocity considered in the integration. This distribution function has a temperature $T_\perp = m(D_{ICRF}+D_{LH})\tau_{SD}$, which reduces to the result of Stix [3] in the limit $D_{LH} \rightarrow 0$. The LH diffusion coefficient can be related to the LH power density absorbed by fast ions by $D_{LH}=\rho_{LH}/3nm$, where n is the fast ion density. In the linear approximation ρ_{LH} is given by

$$\rho_{LH} = \frac{\omega_p^2}{4\pi^{1/2}\omega_{LH}} |\Psi_{RMS}|^2 \left(\frac{E_{RES}}{T_\perp} \right)^{3/2} exp\left(-\frac{E_{RES}}{T_\perp} \right). \qquad (4)$$

Here $\omega_p=(4\pi Z^2 e^2 n/m)^{1/2}$ is the minority ion plasma frequency and $|\Psi_{RMS}|$ is the root mean squared average over $n_{||}$ of the electric field in the LH wave spectrum. In equation 4, absorption of LH power by fast ions reaches its maximum at $E_{RES}/T_\perp = 3/2$, $E_{RES} \geq E_{THR}$. Since $E_{THR}=m_p c^2/2n^2_{\perp MAX}$, we obtain maximum absorption at $n_\perp = 17.62/T_\perp^{1/2}(MeV) \leq n_{\perp MAX}$. In JET deuterium plasmas, the perpendicular proton temperature in typical combined ICRF+LH heating experiments is $0.3 \leq T_\perp(MeV) \leq 0.6$. Thus maximum absorption of LH wave power by ICRF-driven protons is theoretically obtained at $22 \leq n_\perp \leq 33 < n_{\perp MAX}$.

To simulate LH power absorption by an ICRF-driven proton population, the above LH operator was incorporated in the time-dependent PION code [11,12], which self-consistently calculates the ICRF power deposition and the fast ion distribution function. Details of the procedures used for these calculations are given in [11,12]. Figs.3a and 3b [13] show examples of simulated line-integrated perpendicular proton distribution functions in the plasma centre, corresponding to the high energy NPA measurements, for three typical cases: (1) ICRF heating only, $|\Psi_{RMS}|=0$, (2) ICRF+LH heating, $|\Psi_{RMS}| \neq 0$ with $n_{\perp MAX}=20$ and (3) ICRF+LH heating, $|\Psi_{RMS}| \neq 0$, with $n_{\perp MAX}=40$. For illustration, in cases (2) and (3) $\approx 10\%$ of input LH power is assumed to be absorbed by ICRF-driven ions, with the LH deposition profile coinciding with the ICRF deposition profile. In Fig.3a the cross-over between the two distribution functions occurs at $E \geq 2MeV$, whereas in Fig.3b it occurs at $E \approx 1.5MeV$.

The main effect of LH waves on the proton population is to flatten the high-energy tail of their velocity distribution function beyond the threshold energy E_{THR}. In Fig.3a, using $n_{\perp MAX}=20$ corresponding to $E_{THR} \approx 1.2MeV$, the perpendicular temperature of the ICRF-heated protons increases for $E \geq 1.2MeV$ and is slightly ($<10\%$) reduced in the energy range of NPA measurements. In Fig.3b, using $n_{\perp MAX}=40$ corresponding to $E_{THR} \approx 0.3MeV$, the proton temperature is

significantly increased (*>20%*) during combined ICRF+LH heating. These simulations show that a LH wave spectrum with $n_{\perp MAX} \geq 40$ reproduces qualitatively the main features of the measurements.

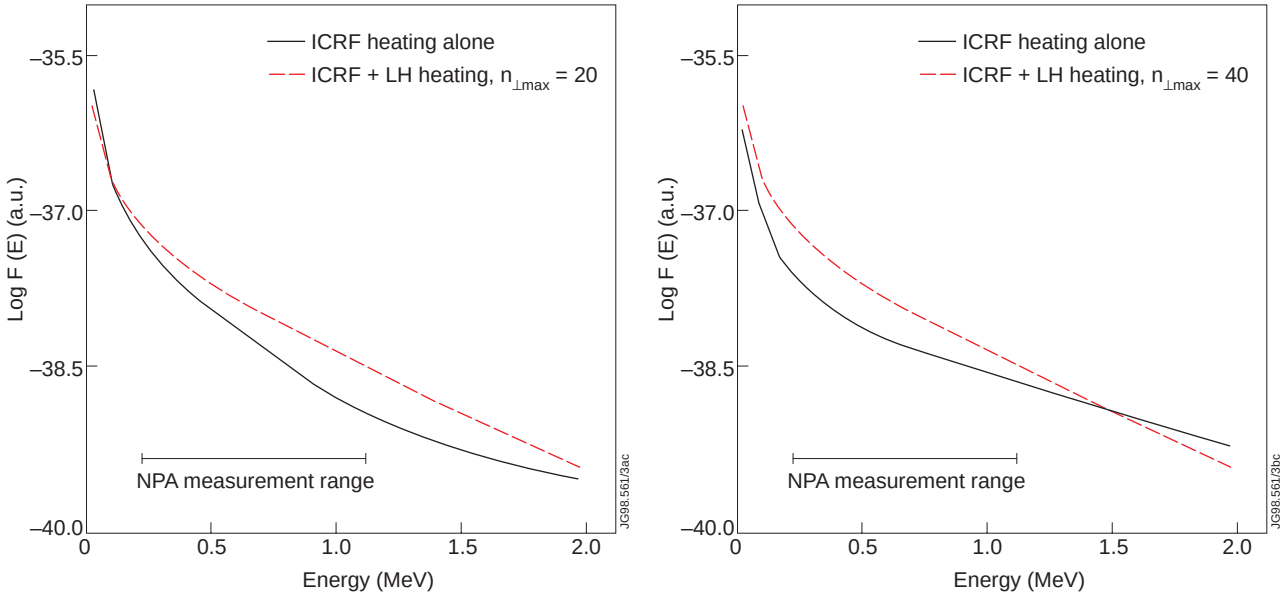

Figure 3. Simulations of the perpendicular proton distribution function during ICRF and LH heating [13]. In Fig.3a, with $n_{\perp MAX}=20$ *corresponding to* $E_{THR}\approx 1.2$MeV, *there is no significant difference in* $T_{\perp}$ *in the energy range of the NPA measurements for* $D_{LH}=0$ *or* $D_{LH}\neq 0$. *In Fig.3b, with* $n_{\perp MAX}=40$ *corresponding to* $E_{THR}\approx 0.3$MeV, $T_{\perp}$ *increases in qualitative agreement with the measurements.*

V. MODIFICATION OF LH DISPERSION RELATION BY ANISOTROPIC HIGH ENERGY PROTONS

These simulations suggest that a LH wave spectrum with $n_{\perp MAX} \geq 40$ could give rise to absorption by the protons as measured. We attribute such modification of the LH wave spectrum to the presence of the protons. The dispersion relation is solved in the LH range of frequencies using cylindrical geometry to describe wave propagation and absorption in non uniform plasmas with parameters corresponding to the JET experiments, with toroidal magnetic field on axis $2.6 \leq B_{\phi 0}(T) \leq 3.4$, LH wave angular frequency $\omega_{LH}=2\pi \times 3.7 \times 10^{9} rad/s$ and parallel refractive index $n_{||}=1.8$. The poloidal component of the confining magnetic field is neglected in our calculations.

We consider a thermal isotropic deuterium plasma and include explicitly minority anisotropic fast protons and fast electrons in the dielectric tensor, therefore adjusting the deuterium concentration to maintain local plasma neutrality. The fast electron population arises due to absorption of LH waves by Landau damping onto thermal electrons, and is responsible for the electron LH current drive. We model the fast proton and fast electron populations using a bi-Maxwellian distribution function

$$f(v_{||},v_{\perp}) = \left(\frac{m}{2\pi}\right)^{3/2} \frac{n}{T_{||}^{1/2} T_{\perp}} exp\left[-\frac{(v_{||}-u_0)^2}{u_{||}^2} - \frac{v_{\perp}^2}{u_{\perp}^2}\right]. \quad (5)$$

Here we use the subscript *e* for thermal electrons, *ef* for fast electrons, *D* for deuterons and *p* for protons. In our calculations we consider $0.05 \le n_p/n_e \le 0.1$, $0.1 \le T_{p\perp}(MeV) \le 0.5$, $T_{p||}/T_{p\perp}=0.1$, $u_{p0}=0$, $n_{ef}/n_e=0.01$, $2 \le u_{ef0}/u_{ef||} \le 4$, $3 \le T_{ef||}/T_e \le 5$, and $T_{ef\perp}/T_{ef||}=0.2$. For such plasma the proton perpendicular beta (the ratio of plasma to magnetic field pressure) is of the order of the total bulk plasma beta in the plasma centre, $\beta_{p\perp} \approx \beta_{BULK} = \beta_D + \beta_e$. Radial profiles are taken as parabolic for the background thermal ions and electrons, as gaussian for the protons and the fast electrons, with half-width at half-maximum corresponding to the width of the ICRF and LH resonance layers. The protons are localised close to the plasma centre [4,5], the fast electrons close to half the minor radius [7,8]. The usual simulations of LHCD in JET [7,8,9] omit the protons and solve the warm plasma dispersion relation, including first order corrections in the plasma temperature and ion-electron collisions.

We consider the full hot-plasma electromagnetic dispersion relation, and solve for the perpendicular component of the refractive index $n_{\perp}$, summing over contributions of the particle species mentioned. The dielectric tensor $\mathbf{D}(\omega,\boldsymbol{k})$ is given by Stix [14] in the form

$$\mathbf{D}(\omega,\mathrm{k}) = \begin{pmatrix} \varepsilon_{xx} - n_{||}^2 & i\varepsilon_{xy} & \varepsilon_{xz} + n_{||}n_{\perp} \\ -i\varepsilon_{xy} & \varepsilon_{yy} - n_{||}^2 - n_{\perp}^2 & i\varepsilon_{yz} \\ \varepsilon_{xz} + n_{||}n_{\perp} & -i\varepsilon_{yz} & \varepsilon_{zz} - n_{\perp}^2 \end{pmatrix}, \quad (6)$$

$$\varepsilon_{ij} = \delta_{ij} + \sum_s \frac{\omega_{ps}^2 e^{-\lambda_s}}{\omega k_{||} u_{s||}} \sum_{q=-\infty}^{\infty} \begin{pmatrix} \frac{q^2 I_q}{\lambda_s} A_q & -q(I_q - I_q')A_q & qI_q B_q \\ q(I_q - I_q')A_q & \left[\frac{q^2 I_q}{\lambda_s} + 2\lambda_s(I_q - I_q')\right]A_q & -(I_q - I_q')B_q \\ qI_q B_q & (I_q - I_q')B_q & 2I_q C_q \end{pmatrix}. \quad (7)$$

Here δ_{ij} is the Kronecker tensor and we use the Onsager symmetry relations. The subscript *s* refers to the different particles' species, the subscript *q* to the cyclotron harmonic number: the cyclotron frequency is positive for ions and negative for electrons. Here I_q and I_q' are the modified Bessel function of the first kind and its derivative, with argument $\lambda = (k_{\perp}u_{\perp}/\Omega)^2/2$. The functions A_q, B_q and C_q are defined for any particles species by

$$A_q = \left(1 - \frac{k_{||}u_0}{\omega}\right) Z_q - \frac{k_{||}u_{||}}{\omega}\left(\frac{T_{\perp}}{T_{||}} - 1\right) W_q \,, \quad (7a)$$

$$B_q = \frac{k_\perp u_{||}}{\Omega}\left\{\frac{q\Omega}{\omega}\frac{u_0}{u_{||}}Z_q - \frac{T_\perp}{T_{||}}\left[1-\frac{q\Omega}{\omega}\left(1-\frac{T_{||}}{T_\perp}\right)\right]W_q\right\}, \quad (7b)$$

$$C_q = \frac{q\Omega}{\omega}\frac{u_0 T_{||}}{u_{||}T_\perp}\left(\frac{u_0}{u_{||}}Z_q - W_q\right) - \frac{\omega - q\Omega}{k_{||}u_{||}}\left[1-\frac{q\Omega}{\omega}\left(1-\frac{T_{||}}{T_\perp}\right)\right]W_q \ . \quad (7c)$$

Here Z_q is the Fried-Conte [16] plasma dispersion function of argument $y_q=(\omega-q\Omega-k_{||}u_0)/k_{||}u_{||}$, and $W_q=-1-y_qZ_q$. All ion species and thermal electrons have $u_0=0$. Fast electrons have $u_0\neq 0$ and can reach energies at which relativistic effects are important: to account for them in a simplified way we use the invariant mass $m_{ef}=\gamma_{ef}m_e$, where $\gamma_{ef}=[1-(u_{ef0}/c)^2]^{1/2}$ is the Lorentz factor and m_e is the electron rest mass. Non-trivial solutions of the dispersion relation are obtained from $Det\{\mathbf{D}(\omega,\mathbf{k})\}=0$ or from the poles in the dispersion relation, giving the resonance condition $k_\perp^2\to\infty$.

The cold-plasma approximation is obtained upon neglecting the minority particles species and taking the limit $T_s\to 0$ for the bulk plasma species: the only surviving elements in the dielectric tensor are (now s refers to bulk electrons and ions)

$$\varepsilon_{xx}=\varepsilon_{yy}=1+\sum_s\frac{\omega_{ps}^2}{\Omega_s^2-\omega^2}=\varepsilon_\perp \ , \quad \varepsilon_{xy}=\sum_s\frac{\omega_{ps}^2\Omega_s}{\omega(\Omega_s^2-\omega^2)}=\varepsilon_{xy0} \ , \quad \varepsilon_{zz}=1-\sum_s\frac{\omega_{ps}^2}{\omega^2}=\varepsilon_{||} \ , \quad (8)$$

and the cold plasma dispersion relation reads

$$Cn_\perp^4 + Bn_\perp^2 + A = 0 \ , \quad (9)$$

$$A=\varepsilon_{||}\left[(\varepsilon_\perp - n_{||}^2)^2 - \varepsilon_{xy0}^2\right] . \quad B=(\varepsilon_\perp+\varepsilon_{||})(n_{||}^2-\varepsilon_\perp)+\varepsilon_{xy0}^2 \ , \quad C=\varepsilon_\perp \ .$$

The warm plasma approximation is obtained keeping first order corrections in the temperature, and the dispersion relation reads

$$Dn_\perp^6 + Cn_\perp^4 + Bn_\perp^2 + A = 0 \ , \ D=-\frac{3u_e^2}{8c^2}\left(\frac{\omega\omega_{pe}}{\Omega_e^2}\right)^2\left[1+\frac{\gamma_{ef}^2 n_{ef}T_{ef\perp}}{n_eT_e}\left(1-\frac{k_{||}u_{ef0}}{\omega}\right)^2\right]-\sum_i\frac{3u_{i\perp}^2}{2c^2}\frac{\omega_{pi}^2}{\omega^2} \ . \quad (10)$$

Here the subscript i refers to the ion species, and the coefficient D is a perturbation to the cold plasma dispersion relation, $|D|<<\{|A|,|B|,|C|\}$. The contributions from the protons and the fast electrons have been included in the correction factor D.

For the purpose of solving the dispersion relation we use the code ZERINT [15], which was developed for the solution of general, complex algebraic equations of the form $F(z,p)=0$, where F and z are complex and p is a set of real parameters. A number of iterative numerical methods are provided within the program to determine the accurate location of the zeros of F. The most generally useful of these is based on Muller's method, where three neighbouring

points are used to fit a quadratic form derived from the local Taylor expansion of the function. The new approximation to the required root is then calculated analytically from this interpolating expansion. The point with the highest residual is then replaced by the latest approximation and the process repeated until a prescribed residual has been reached. In the neighbourhood of a zero, Muller's method exhibits nearly-quadratic convergence properties, but fails for a *funnel* zero, that is when the function is very large except for a very small *hole* which contains the root. Two further methods are provided which can prove useful in a few circumstances. The first is similar to Muller's method except that the local functional form is taken to be bilinear, which can be of some advantage when roots are very close to poles of F. Secondly, a technique involving the Cauchy residue theorem can be employed to determine the number of roots in a closed contour. Provided no poles are present and the roots are not degenerate, an estimate of their positions can be obtained, and this method can be used to overcome the difficulties due to *funnel* zeros. There are a number of safeguards implemented in ZERINT so that divergent behaviour can be quickly detected and corrected.

We find that the presence of the protons affects the dispersion of waves in the LH range of frequencies by introducing an ensemble of hot-plasma wave modes [17]. For a thermal plasma without the proton population, the slow and fast waves are found with $n_{\perp MAX} \leq 20$ using the cold and warm plasma approximation; these solutions are continuous in ω_{LH}/Ω_p. For a thermal plasma containing the proton population, solutions of the dispersion relation are found with $n_{\perp MAX} \geq 40$ in addition to the (cold and warm plasma) slow and fast waves. These hot-plasma solutions show a discrete resonant structure in ω_{LH}/Ω_p for given background plasma and $n_{||}$. Figs. 4a and 4b show solutions of the dispersion relation in the LH range of frequencies with $n_e=3x10^{19}m^{-3}$, $n_D/n_e=0.89$, $n_p/n_e=0.1$, $n_{ef}/n_e=0.01$, $T_e=T_D=5keV$, $T_{p\perp}=0.3MeV$, $T_{p\perp}/T_{p||}=10$, $(u_{ef0}/u_e)^2=10$, $T_{ef||}=30keV$, $T_{ef||}/T_{ef\perp}=5$, $n_{||}=1.8$, $\omega_{LH}=2\pi x3.7rad/s$. The slow and fast wave modes, below the dashed line, have $n_{\perp MAX}<20$ and are continuous in the wave harmonic number $q=\omega_{LH}/\Omega_p$. Hot plasma solutions with $n_{\perp MAX}>30$ are found for given $n_{||}$ only in resonant bands (the three vertical series above the dashed line) around discrete values of $q=q_0 \pm \Delta q$, with $q_0=\{74,86,98\}$ and $\Delta q=2$. The resonance width $\Delta n_\perp/n_\perp<0.1$ of these hot-plasma modes increases with $T_{p\perp}$. Similar properties of the dispersion relation are found in the range of plasma parameters corresponding to the experiments reported here.

The properties of the solutions of the LH dispersion relation are summarised as follows:

(a) for a thermal deuterium plasma, using either the cold or warm plasma approximation, the slow and the fast wave roots of the dispersion relation are found with $n_{\perp MAX}<18$;

(b) for a thermal deuterium plasma containing a minority anisotropic high energy proton population $\beta_{p\perp} \approx \beta_{BULK}$ in the plasma centre, an ensemble of hot-plasma wave modes is found in the plasma centre with $n_{\perp MAX}>40$;

(c) hot plasma modes are found with similar properties in the range of parameters corresponding to the experiments with combined ICRF+LHCD heating, reported in Section 1;

(d) hot-plasma modes show a discrete resonant structure with respect to the wave harmonic number $q=\omega_{LH}/\Omega_p$, suggesting cyclotron-like damping of LH waves on the protons;

(e) for given background plasma, values of ω_{LH}/Ω_p and $n_{||}$ exist for which such hot-plasma solutions are not found, thus significantly weakening absorption of LH waves by the protons.

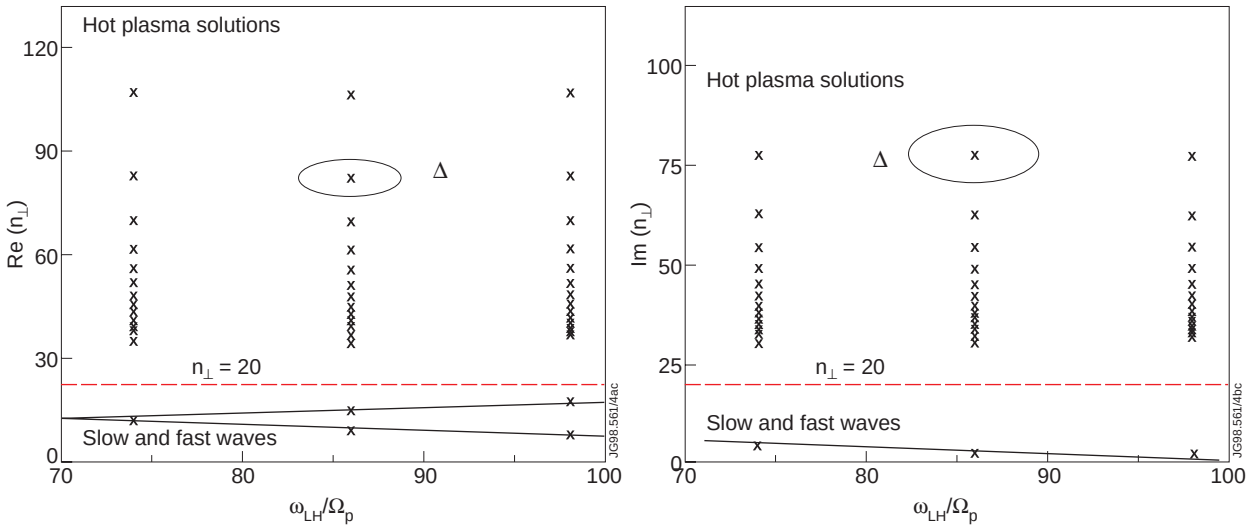

Figure 4. Solutions of the LH dispersion relation with $n_e=3\times10^{19}m^{-3}$, $n_D/n_e=0.89$, $n_p/n_e=0.1$, $n_{ef}/n_e=0.01$, $T_e=T_D=5$keV, $T_{p\perp}=0.3$MeV, $T_{p\perp}/T_{p||}=10$, $(u_{ef0}/u_e)^2=10$, $T_{ef||}=30$keV, $T_{ef||}/T_{ef\perp}=5$, $n_{||}=1.8$, $\omega_{LH}=2\pi\times3.7$rad/s, *as function of the harmonic number* $q=\omega_{LH}/\Omega_p$ *for* $70\le q\le100$, *corresponding to* $2.4\le B_{\phi0}(T)\le3.5$. *The slow and fast wave modes, below the dashed line, have* $n_{\perp MAX}<20$ *and are continuous in* ω_{LH}/Ω_p. *Hot plasma roots with* $n_{\perp MAX}>30$ *(above the dashed line) are found only in resonant bands around discrete values of the harmonic number for given* $n_{||}$: $q=q_0\pm\Delta q$, $q_0=\{74,86,98\}$ *and* $\Delta q=2$. *The resonance width* $\Delta n_\perp/n_\perp<0.1$ *of the hot plasma wave modes increases with* $T_{p\perp}$. *Note that in Fig.4b for the slow and the fast wave* $\mathrm{Im}(n_\perp)$ *is vanishingly small, whereas hot plasma wave modes have large positive* $\mathrm{Im}(n_\perp)$, *implying strong wave damping.*

Using these results for $n_\perp$, we computed the slow wave accessibility to the hot-plasma solutions across the normalised minor radius *r/a*, as shown in Fig.5. Radial profiles are taken as parabolic for background thermal ions and electrons, gaussian for minority non-thermal protons and electrons, with half-width at half-maximum corresponding to the half width of the ICRF and LHCD resonance layers. The sum over cyclotron harmonics is truncated at $q_{BES}=c_0(A/Z^2)T_\perp(keV)$: c_0 is an empirical constant depending on the desired numerical accuracy. Stability in the iteration procedure is obtained with relative accuracy $\le10^{-8}$ using $c_0=0.5$ for ions and $c_0=0.2$ for electrons.

We obtain an initial guess for $n_{\perp HOT}$ using the cold plasma approximation, and we iterate the procedure until convergence is locally found for the slow wave mode: then we track this slow wave root of the dispersion relation across the plasma cross-section. Mode conversion to hot plasma wave modes with $n_{\perp HOT}>>n_{\perp COLD}$ is found close to the plasma centre due to the fast protons and close to half the minor radius due to the fast electrons if $n_{||}$ is below the condition for accessibility to the slow wave, $n_{||}<n_{||MC}$.

Fig. 5 show the results of our calculations. For the plasma parameters of Fig.4, we find that $n_{||MC} \approx 1.9$, and no confluence is possible between the slow and fast wave modes, since the critical parallel refractive [14] $n_{||CRIT} < 0$ for such plasma. These two mode conversion regions are very narrow, approximately $0.1x(r/a)$, and their position coincides with the peak in the fast particle perpendicular beta. Outside these regions the slow wave root returns to its cold plasma value, and we do not follow further the hot-plasma wave modes. For $n_{||} > n_{||MC}$ no mode conversion is found and the perpendicular refractive index differs nowhere across the plasma cross-section by more than 10% from the hot and cold plasma solutions.

Work is now underway in an attempt to develop an approximate analytic theory of the above numerical results in order to shed further light on the role of the energetic minority protons and the fast current carrying electrons. Preliminary analysis indicates that these hot-plasma wave modes are Bernstein-like waves: the non thermal minority populations provide the stronger ion damping to account for the enhanced ion absorption of the LH waves. Their contribution is effective only up to a certain value of $k_{||}$. This result is in qualitative agreement with our numerical calculations and with measurements of $f_p(E)$ during combined ICRF+LH heating experiments in which no coupling of LH waves to the protons seems to occur. For these cases, our calculations indicate that $0.8 \leq n_{||MC} \leq 1.3$, well below the launched value of $n_{||}$, so we would not expect any mode conversion to occur.

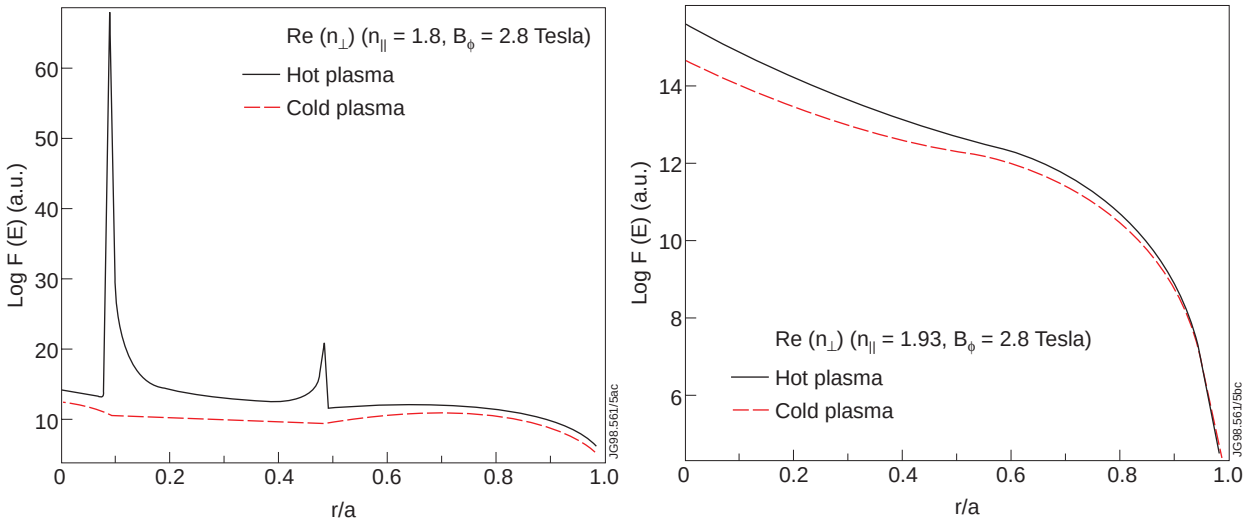

Figure 5. Hot plasma slow wave root of the LH dispersion relation as a function of the normalised minor radius r/a *with the same plasma parameter as in Fig.4. In Fig.5a modes with* $n_{\perp HOT} >> n_{\perp COLD}$ *are found near the plasma centre due to the fast protons and near half the minor radius due to the fast electrons. In Fig.5b wave modes with* $n_{\perp HOT} >> n_{\perp COLD}$ *are not found because* $n_{||}$ *is now above the accessibility condition to the slow wave,* $n_{||MC} \approx 1.9$.

Work is in progress on the understanding of the critical parallel refractive index below which mode conversion is found between the slow wave and the hot-plasma modes. We obtain numerically that the value of $n_{||MC}$ is always above $n_{||CRIT}$, depends strongly on the bulk plasma density for $\beta_{p\perp}/\beta_{BULK} \sim 1$, increasing for larger densities, and is much less sensitive to the mag-

netic field and bulk plasma temperature. If $\beta_{p\perp}/\beta_{BULK}<<1$, no hot-plasma modes with $n_\perp \geq 40$ are found in the plasma centre irrespective of $n_{||}$.

Finally, following the method developed by Woods, Cairns and Lashmore-Davies [18], we compute the dispersion relation $\omega=\omega(k_\perp)$ for the hot-plasma modes across the normalised minor radius, thus avoiding ambiguities about the direction of the group velocity of these wave modes. We consider $\omega=\omega_1+\delta\omega$, where ω_1 is the launched LH wave angular frequency (corresponding to the slow wave) and $\delta\omega$ is the (complex) perturbation to ω_1 induced by the fast protons (near the plasma centre) and the fast electrons (near half the minor radius). We compute locally $\delta\omega$ using a fourth order equation for low-frequency waves derived under the condition $\{|\Omega_e|,\omega_{pe}\}>>\omega\approx\omega_{LH}$

$$\omega_{pe}^2(A+B\omega^2+C\omega^4)=0=\omega_{pe}^2(\omega^2-\omega_1^2)(\omega^2-\omega_2^2)\,, \tag{11}$$

$$A=\left(k^2c^2+\omega_{pi}^2\right)\left(k_{||}^2c^2+\omega_{pi}^2\right)+k^4c^4\frac{\omega_{pi}^2}{\omega_{pe}^2}\,,\qquad C=\left(1+\frac{\omega_{pe}^2}{\Omega_e^2}\right)^2\,,$$

$$B=-\frac{\omega_{pe}^2}{\Omega_e^2}\left(k_\perp^2c^2+\omega_{pe}^2\right)-\left(1+\frac{\omega_{pe}^2}{\Omega_e^2}\right)\left[2\left(k_{||}^2c^2+\omega_{pi}^2\right)+k_\perp^2c^2\left(1+\frac{k_\perp^2c^2}{\omega_{pe}^2}\right)\right].$$

We consider $\omega_1\approx\omega_{LH}<<\omega_2\approx\omega_{pe}$, and we expand the conductivity tensor elements as the sum of the cold bulk plasma and fast minority species contributions

$$\varepsilon_{xx}=\varepsilon_\perp+\varepsilon_{xx}^{(f)}\,.\qquad \varepsilon_{xy}=\varepsilon_{xy0}+\varepsilon_{xy}^{(f)}\,,\qquad \varepsilon_{xz}=\varepsilon_{xz}^{(f)}\,,$$

$$\varepsilon_{yy}=\varepsilon_\perp+\varepsilon_{yy}^{(f)}\,,\qquad \varepsilon_{yz}=\varepsilon_{yz}^{(f)}\,,\qquad \varepsilon_{zz}=\varepsilon_{||}+\varepsilon_{zz}^{(f)}\,.$$

Here the superscript *(f)* refers to both the fast proton and electron species. We then derive the following equation for the perturbation $\delta\omega/\omega_1$:

$$\begin{aligned}\left(\frac{\delta\omega}{\omega_1}\right)_{NL}^{(f)}=\frac{\omega_1^4}{2\omega_{pe}^2\left(\omega_2^2-\omega_1^2\right)}\Big\{&\left(\varepsilon_{||}-n_\perp^2\right)\left(\varepsilon_{yy}-n^2\right)\varepsilon_{xx}^{(f)}-\left(\varepsilon_{||}-n_\perp^2\right)\left(2\varepsilon_{xy0}+\varepsilon_{xy}^{(f)}\right)\varepsilon_{xy}^{(f)}+\\&+\left[\varepsilon_\perp\left(\varepsilon_{||}-n_\perp^2\right)-n_{||}^2\varepsilon_{||}\right]\varepsilon_{yy}^{(f)}+\left[\left(\varepsilon_{yy}-n^2\right)\left(\varepsilon_{xx}-n_{||}^2\right)-\varepsilon_{xy}^2\right]\varepsilon_{zz}^{(f)}+\\&-\left(\varepsilon_{yy}-n^2\right)\left(\varepsilon_{xz}^{(f)}+2n_{||}n_\perp\right)\varepsilon_{xz}^{(f)}-\left[\left(\varepsilon_{xx}-n_{||}^2\right)\varepsilon_{yz}^{(f)}+2\varepsilon_{xy}\left(\varepsilon_{xz}^{(f)}+n_{||}n_\perp\right)\right]\varepsilon_{yz}^{(f)}\Big\}\end{aligned}\,. \tag{12}$$

In equation (12) we note that the cold plasma conductivity tensor elements $\{\varepsilon_\perp,\varepsilon_{xy0},\varepsilon_{||}\}$ represent the dominant contribution, thus we can neglect quadratic terms in the fast particles' contribution and obtain the following linearised equation for the perturbation $\delta\omega/\omega_1$:

$$\left(\frac{\delta\omega}{\omega_1}\right)^{(f)}_{LIN} = \frac{\omega_1^4}{2\omega_{pe}^2\left(\omega_2^2-\omega_1^2\right)}\left\{\left(\varepsilon_{||}-n_\perp^2\right)\left(\varepsilon_\perp-n^2\right)\varepsilon_{xx}^{(f)} - 2\varepsilon_{xy0}\left(\varepsilon_{||}-n_\perp^2\right)\varepsilon_{xy}^{(f)} + \right.$$
$$+\left[\varepsilon_\perp\left(\varepsilon_{||}-n_\perp^2\right)-n_{||}^2\varepsilon_{||}\right]\varepsilon_{yy}^{(f)} + \left[\left(\varepsilon_\perp-n^2\right)\left(\varepsilon_\perp-n_{||}^2\right)-\varepsilon_{xy0}^2\right]\varepsilon_{zz}^{(f)} + \quad . \qquad (13)$$
$$\left.-2n_{||}n_\perp\left[\left(\varepsilon_\perp-n^2\right)\varepsilon_{xz}^{(f)}+\varepsilon_{xy0}\varepsilon_{yz}^{(f)}\right]\right\}$$

The perturbation produced by the protons to the launched slow wave mode is vanishingly small outside the ICRF resonance layer: we then compute the average value of $\delta\omega/\omega_1$ in this region. Fig.6 shows the results of our calculations. We find that the correction is small, thus justifying use of perturbative theory and the neglect of quadratic terms, is quite insensitive to the value of the launched $n_{||}$ and has a negative imaginary part, corresponding to damping by the protons. The parallel refractive index is then crucial in determining the accessibility of the (launched) slow wave to the hot plasma modes, but it plays little role in further determining the properties of these hot plasma modes once they have access to the slow wave.

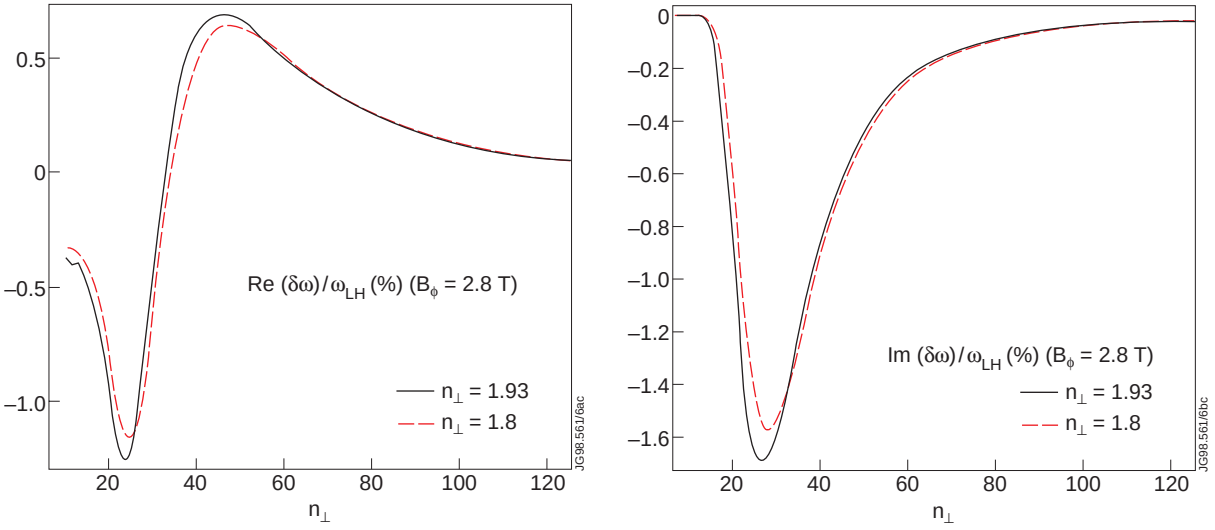

Figure 6. Real (Fig.6a) and imaginary (Fig.6b) parts of hot-plasma wave frequency induced by the protons as perturbation to the launched LH frequency, averaged over the ICRF resonance layer, with the same plasma parameters as Fig.4. The correction is small, thus justifying use of perturbative theory and neglect of quadratic terms, and is quite insensitive to the value of $n_{||}$.

VI. POWER ABSORPTION BY FAST PROTONS

We compute, using the hot plasma roots of the LH dispersion relation, Fig.4, the fraction of LH power absorbed by the protons averaging over the ICRF resonance layer assuming single pass absorption, $P_{ABS}=P_{LH}exp(2\omega_I\tau)$. Here ω_I is the imaginary part of the frequency $\omega=\omega_1+\delta\omega$, $\delta\omega$ is the perturbation induced by the high energy protons computed in Section 5 using equation (13), and τ is the wave transit time across the ICRF resonance layer.

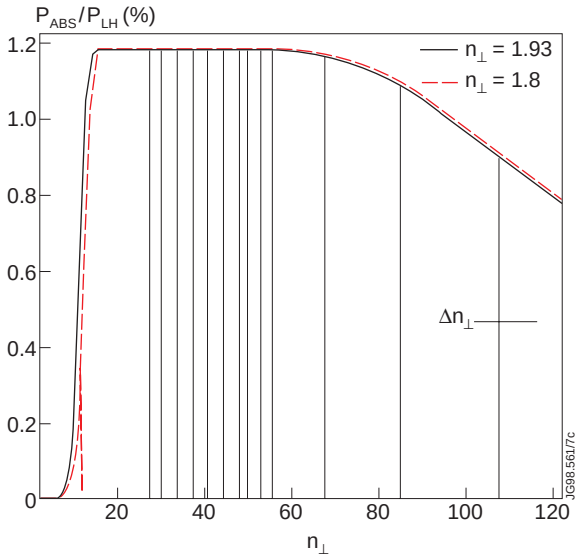

Figure 7. LH power absorbed by the protons as function of $n_\perp$*, for the same plasma as in Fig.4. The full vertical lines at* $n_\perp > 30$ *indicate the hot-plasma wave modes induced in the plasma centre by the protons. For clarity their resonance width* $\Delta n_\perp / n_\perp < 0.1$ *is shown only for one of them. The dashed vertical line at* $n_\perp \approx 16$ *indicates the cold plasma slow wave. Note that no significant difference is found for values of* $n_\parallel$ *above and below* $n_{\parallel MC}$.

Fig.7 shows the result of such a procedure. Summing over all the hot plasma wave modes, including their resonance width $\Delta n_\perp$, we find that *≈30%* of the input LH power is absorbed by the protons. For the cold-plasma slow wave mode, only *≈5%* of input LH power is damped onto the protons. It is worthwhile noting that maximum coupling of LH waves to the protons is found for $20 \le n_\perp \le 60$, in good agreement with the linear approximation to the absorbed power density computed using the QL diffusion coefficients, equation (4). This result further validates our analytical approach to the numerical calculations.

VII.CONCLUSIONS

We have shown experimental evidence of interaction between LH waves and ICRF-heated protons in JET using NPA measurements of the proton distribution function in the range $0.3 \le E(MeV) \le 1.1$. The coupling was observed for driven as well as for slowing-down protons. Energy balance considerations give larger proton heating during application of combined ICRF and LH power than would be obtained with ICRF heating alone. We deduce that ≈30% of LH input power is coupled directly to the protons, with no significant dependence on background plasma parameters. We have tested, using 1D numerical Fokker-Planck modelling, a conjecture that this coupling is effected by modifications of LH dispersion in the plasma, and the experimental observations are qualitatively reproduced using $n_{\perp MAX} \ge 40$. We investigated reasons for the existence of wave modes with $n_{\perp MAX} \ge 40$ by solving the hot-plasma dispersion relation in the LH range of frequencies, including LHCD-driven electrons and ICRF-driven protons, using

cylindrical geometry for the wave propagation and absorption. Solutions of the dispersion relation with $n_{\perp MAX} \geq 40$ are found in the LH range of frequencies in the plasma centre when the proton population is added to a thermal deuterium plasma with $\beta_{p\perp} \approx \beta_{BULK} = \beta_D + \beta_e$. Such hot-plasma wave modes are not found if $\beta_{p\perp}/\beta_{BULK} << 1$. These modes correspond to LH waves damping on the protons and show a discrete cyclotron-like resonant structure with respect to ω_{LH}/Ω_p for given background plasma and $n_{||}$. We interpret these hot-plasma wave modes as Bernstein-like waves coupled to the protons. The protons provide the stronger ion damping to account for the enhanced ion absorption of the LH waves up to a maximum value for $k_{||}$. This could explain certain experiments where no absorption of LH waves by the protons was observed. Cold plasma modes with $n_{\perp MAX} \leq 20$ damp only ≈5-10% of LH input power onto the proton population, consistent with the usual simulations of LHCD in JET. Hot plasma modes with $n_{\perp MAX} \geq 40$ damp ≈30% of the LH input power onto the protons, consistent with measurements and simulations of the proton distribution function. Hot plasma wave modes are not found if $\beta_{p\perp} << \beta_{BULK}$. For $\beta_{p\perp} \approx \beta_{BULK}$, hot plasma wave modes are not found on increasing the launched parallel wavenumber above the critical value for accessibility to the slow wave or, alternatively, by adjusting the magnetic field and the launched LH frequency. This critical parallel refractive index shows for $\beta_{p\perp} \approx \beta_{BULK}$ a very strong dependence on the electron density, increasing for larger densities, and is much less sensitive to the magnetic field and bulk plasma temperature. This result is therefore promising for maximising efficiency of LHCD in plasmas containing high energy charged fusion products and give useful insights into the alpha-channelling scheme proposed by Fisch [19].

Work is now in progress (a) to give a more complete physical interpretation to our numerical solution of the dispersion relation in the LH range of frequencies, and (b) to study the interaction of LH waves with charged fusion products in reactor relevant conditions, such as those foreseen for ITER.

ACKNOWLEDGEMENTS

The authors would like to thank Professor Malcolm Haines for advice and encouragement of this work. The authors are also indebted to Dr.Xavier Litaudon for clarifying discussions on lower hybrid wave propagation in fusion plasmas. The work of UKAEA Fusion authors was jointly supported by the UK Department of Trade and Industry and EURATOM.

REFERENCES

[1] A.A.Korotkov, A.Gondhalekar 1994, *Proc. 21st Eur. Conf.*, Montpellier, **18B**, 266.

[2] A.A.Korotkov, A.Gondhalekar and A.J.Stuart 1997, *Nucl. Fus.* **37**, 35.

[3] T.H.Stix 1975, *Nucl. Fus.* **15**, 737.

[4] K.G.McClements, R.O.Dendy and A.Gondhalekar 1997, *Nucl. Fus.* **37**, 473.

[5] D.Testa, W.G.F.Core and A.Gondhalekar 1998, *Interpretation of measurements of hydrogen isotope ion energy distribution function during multispecies minority ICRF heating of deuterium plasmas in JET*, submitted to Nuclear Fusion, October 1998. D.Testa and A. Gondhalekar 1998, *Fast Ion Densityergy Neutral Particle Analysis in JET,* in preparation.

[6] C.F.F.Karney 1978, *Phys. Fluids* **21**, 1584.

[7] Y.F.Baranov, A.Ekedahl, P.Froissard, C.Gormezano et al 1996, *Nucl. Fus.* **36**, 1031.

[8] A.Ekedahl, Y.Baranov et al 1997, *Profile Control Experiments in JET using off-axis Lower Hybrid Current Drive*, submitted for publication in Nuclear Fusion.

[9] M.C.Ramos de Andrade et al 1994, *Plasma Phys. Control. Fusion* **36**, 1171.

[10] E.Barbato and F.Santini 1991, *Nucl. Fus.* **31,** 673.

[11] L.G.Eriksson, T.Hellsten and U.Willén 1993, *Nucl. Fus.* **33**, 1037.

[12] L.-G.Eriksson and T.Hellsten 1995, *Phys. Scr.* **55**, 70.

[13] D.Testa, A.Gondhalekar et al 1997, *Proc. 24th Eur. Conf.*, Berchtesgaden, **21A**, 129.

[14] T.H.Stix, *Waves in plasmas*, American Institute of Physics, New York,1992.

[15] Terry Martin, Culham Science Centre, private communication.

[16] B.D.Fried and S.D.Conte, *The plasma dispersion function*, Academic Press, New York, 1961.

[17] D.Testa, C.N.Lashmore-Davies et al 1998, *Proc. 2nd Eur. Top. Conf. on RF Heating and Current Drive in Fusion Devices*, Brussels, **22A**, 197.

[18] A.M.Woods, R.A.Cairns and C.N.Lashmore-Davies 1986, *Phys. Fluids* **29**, 3719.

[19] N.J.Fisch and J.-M.Rax 1992, *Phys. Rev. Lett.* **69**, 612.